



HAL
open science

Sustained-release microparticle dry powders of chloramphenicol palmitate or thiamphenicol palmitate prodrugs for lung delivery as aerosols

Siti Nani Nurbaeti, Julien Brillault, Frédéric Tewes, Jean-Christophe Olivier

► To cite this version:

Siti Nani Nurbaeti, Julien Brillault, Frédéric Tewes, Jean-Christophe Olivier. Sustained-release microparticle dry powders of chloramphenicol palmitate or thiamphenicol palmitate prodrugs for lung delivery as aerosols. *European Journal of Pharmaceutical Sciences*, 2019, 138, pp.105028. 10.1016/j.ejps.2019.105028 . hal-02477590

HAL Id: hal-02477590

<https://hal.science/hal-02477590v1>

Submitted on 20 Jul 2022

HAL is a multi-disciplinary open access archive for the deposit and dissemination of scientific research documents, whether they are published or not. The documents may come from teaching and research institutions in France or abroad, or from public or private research centers.

L'archive ouverte pluridisciplinaire **HAL**, est destinée au dépôt et à la diffusion de documents scientifiques de niveau recherche, publiés ou non, émanant des établissements d'enseignement et de recherche français ou étrangers, des laboratoires publics ou privés.



Distributed under a Creative Commons Attribution - NonCommercial 4.0 International License

1 **Sustained-release microparticle dry powders of chloramphenicol**
2 **palmitate or thiamphenicol palmitate prodrugs for lung delivery as**
3 **aerosols.**

4 **Siti Nani Nurbaeti^{1,2}, Julien Brillault^{1,2}, Frédéric Tewes^{1,2}, Jean-Christophe Olivier^{1,2}**

5 ¹INSERM, U 1070, Pôle Biologie Santé, 1 rue Georges Bonnet, TSA 51106, 86073 Poitiers
6 Cedex 9, France

7 ²Université de Poitiers, Faculté de Médecine et Pharmacie, 6 rue de la Milétrie, TSA 51115,
8 86073 Poitiers Cedex 9, France

9 #Address correspondence to Julien Brillault, Pôle Biologie Santé, Bâtiment B36/B37, INSERM
10 U1070, 1 Rue Georges Bonnet, TSA 51106, 86073 POITIERS Cedex 9, France. Email:
11 Julien.brillault@univ-poitiers.fr

12

13 **Abstract**

14 The purpose of this study was to design inhalable sustained-release nanoparticle-in-
15 microparticles, *i.e.* nano-embedded microparticles, for the lung delivery of chloramphenicol
16 or thiamphenicol as aerosols. The palmitate ester prodrugs of the two antibiotics were used
17 to prepare PLGA-based nanoparticles or to form pure prodrug nanoparticles. Prodrug-loaded
18 PLGA nanoparticles or pure prodrug nanoparticles were prepared using the emulsion-solvent
19 evaporation method. Dry microparticle powders for inhalation were then produced by
20 spray-drying the nanoparticle suspensions supplemented with lactose as a bulking agent and
21 L-leucine as a dispersing enhancer. Examined under the scanning electron microscopy, the
22 obtained microparticles appeared to be spherical and shriveled, with no crystal-like
23 structures. Drug loading was satisfactory (14 to 34 % (m/m)) and the aerodynamic properties
24 determined with a Next Generation Impactor were appropriate for lung delivery, with mass
25 median aerodynamic diameters close to 3 µm. The *in vitro* release profiles showed that
26 sustained released was achieved with these formulations, with an almost complete release
27 over 14 days.

28 *Keywords:* chloramphenicol, thiamphenicol, aerosol, lung delivery, antimicrobial, palmitate
29 prodrug, PLGA.

30

31 **1. Introduction**

32

33 Chloramphenicol (CHL) and thiamphenicol (THA) are antibiotics of the amphenicol class that
34 possess similar broad spectra of activity against Gram positive and Gram negative bacteria
35 (Eliakim-Raz et al., 2015; Serra et al., 2007). Commonly used in the past due to its broad
36 spectrum and its good diffusion into tissues, chloramphenicol was reported to cause rare,
37 irreversible and fatal idiosyncratic aplastic anaemia, which was attributed to the nitroso-
38 chloramphenicol metabolite responsible for DNA damage (Dinos et al., 2016; Ferrari, 1984).
39 Possessing a methyl sulfonyl group in place of the nitro group thiamphenicol was not
40 associated with such a lateral effect (Ferrari, 1984; Yunis, 1984). Both chloramphenicol and
41 thiamphenicol are however responsible for reversible dose-dependent bone marrow
42 suppression in the case of prolonged systemic treatments (more than 7 days) (Eliakim-Raz et
43 al., 2015; Ferrari, 1984). In the advanced countries, they have therefore been replaced in
44 clinical practice with less toxic antibiotics, and their use is recommended as the second line
45 treatments of life-threatening infections that do not respond to other antibiotics (Eliakim-
46 Raz et al., 2015). Chloramphenicol is inexpensive, and is still widely used as topical
47 preparations, e.g. in eye drops for the prevention and treatment of superficial eye infections,
48 or as oral tablets or capsules or pediatric suspension in low-income countries (Lam et al.,
49 2002). Though potentially useful for the treatment of life-threatening infections resistant to
50 other antibiotics, chloramphenicol and thiamphenicol are not available world-wide and are
51 considered as “forgotten” antibiotics in advanced countries (Pulcini et al., 2017). In
52 particular, CHL and THA have been proposed to treat multidrug-resistant pulmonary
53 bacterial infections. Their direct administration into the lungs as therapeutic aerosols should
54 be considered to increase treatment efficiency and minimize whole body exposure
55 responsible for adverse effects, particularly in the case of prolonged treatments.
56 Thiamphenicol, in the form of its glycinate ester prodrug, was administered as an aerosol in
57 oncological patients with respiratory infections and was effective in more than 95% of the
58 patients (Macchi et al., 2011).

59 Due to their lipophilicity both CHL and THA (ALOGPS predicted logP = 1.15 and 0.33,
60 respectively (Tetko et al., 2005)) were shown to have a high permeability across a broncho-
61 alveolar epithelium model made of Calu-3 cell line (Nurbaeti et al., 2018), in consistency with
62 the rapid intestinal absorption reported in human PK studies after oral administration
63 (Ambrose, 1984; Ferrari, 1984). Due to their high apparent epithelial permeability, the
64 pulmonary administration of CHL or THA will not improve lung exposure to these antibiotics
65 compared to systemic administration. Therefore, in order to improve lung exposure to CHL
66 or THA after their aerosolization, it is relevant to formulate them as sustained release drug
67 delivery systems. Indeed, in previous works, we showed that antibiotics-loaded PLGA
68 microspheres with sustained-release properties permitted to dramatically increase the
69 concentration of high-permeability antibiotics in the pulmonary epithelial lining fluid over a
70 prolonged time period (more than 72 h), compared to an intratracheally nebulized solution
71 or an IV infusion (Doan et al., 2013; Gaspar et al., 2016). In preliminary experiments, the
72 formulation and the preparation of CHL- or THA-loaded PLGA microspheres using the solvent
73 evaporation method resulted in an insufficient drug loading (from 1 to 5% (w/w)) (data not
74 shown). Previous studies showed that using lipophilic prodrugs dramatically increased the
75 nanoparticle drug content compared to the parent drug and prolong the release time
76 (Gomez-Gaete et al., 2008; Han et al., 2015). Lipophilic palmitate esters of chloramphenicol
77 or of thiamphenicol are available. Chloramphenicol palmitate (CHLP) was synthesized in the
78 past as a tasteless prodrug for oral administration in children. Different from
79 chloramphenicol it is poorly absorbed, but it is quickly and almost completely hydrolyzed
80 into the parent drug by esterases in the small intestine, which results in a CHL bioavailability
81 similar to oral dosage forms of CHL (Ambrose, 1984). CHLP is marketed as a pediatric oral
82 suspension in some countries. In the present work, lipophilic palmitate esters of CHL or of
83 THA were formulated as dry nano-embedded microparticle powders for inhalation based on
84 the nanoparticle aggregation process through the spray-drying of nanoparticle aqueous
85 suspensions, based on methods described previously (Gomez-Gaete et al., 2008; Ruge et al.,
86 2016; Torge et al., 2017). The nanoparticles were made with the prodrugs and PLGA polymer
87 or with the prodrugs only using the solvent evaporation method and were then spray-dried
88 in a solution of lactose and L-leucine in order to obtain nano-embedded microparticle dry
89 powders. Once delivered by inhalation, the nano-embedded lactose microparticles are
90 expected to dissolve and release the nanoparticles in the lungs. Nanoparticles will then

91 gradually release the prodrugs that will eventually be hydrolyzed by lung lipases into the
92 active parent drugs (Camps et al., 1991).

93

94 **2. Materials and methods**

95 **2.1. Materials**

96 Thiamphenicol (THA) (98% pure), Chloramphenicol (CHL) (99% pure), Resomer® RG 502 H
97 (PLGA 50:50, MW: 7,000–17,000, acid terminated), alpha-lactose monohydrate (purity ≥
98 99%), L-leucine and lipase from porcine pancreas were purchased from Sigma-Aldrich (St.
99 Quentin Fallavier, France). Chloramphenicol palmitate (CHLP) (Fig. 1) was purchased from
100 Chem-Impex International, Inc. (Wood Dale, IL, USA). Thiamphenicol palmitate (THAP) (Fig.
101 1) was obtained from Abcam (Paris, France). Rhodoviol 4/125 (polyvinylalcohol, degree of
102 hydrolysis of 88%) was purchased from Prolabo (Paris, France). Purified water was produced
103 with a milli DI™ Millipore system and HPLC quality grade water used for HPLC analysis was
104 purchased from Carlo Erba (Val de Reuil, France). Hank's Balanced Salt Solution (HBSS) was
105 obtained from PAN Biotech GmbH (Aidenbach, Germany).

106

107 **2.2. Methods**

108 **2.2.1. Nanoparticle preparation and characterization**

109 Nanoparticles were prepared by an emulsion-solvent evaporation method. For the
110 preparation of the prodrug-loaded PLGA nanoparticles, a solution of PLGA (100 mg) and
111 prodrug (100 mg) in 20 ml of ethyl acetate (EA) was vortex mixed with 80 ml of an aqueous
112 solution of polyvinylalcohol (0.5% w/v) supplemented with 4.68 ml of EA. Then, in an ice
113 bath, the mixture was subjected to magnetic stirring and ultrasonication for 6 min using a
114 probe sonicator (Branson Sonifier 450) set at 20% maximum power. For the preparation of
115 the prodrug nanoparticles, 200 mg of prodrug were dissolved in EA and processed as above.
116 EA was evaporated off under vacuum at 30°C during 1 h using a rotary evaporator. Volume
117 was adjusted to 80 ml with water and the suspension was filtered on a Fischerbrand glass
118 microfibre filter (2.7 µm porosity). The mean diameter of the nanoparticle volume-
119 weighted distribution (D_v) was determined in purified water by laser light diffraction
120 (Microtrac® X100 particle size analyzer). The width of particle size distribution, or span, was
121 calculated according to: $\text{span} = (d_{90} - d_{10}) / d_{50}$, where d_{10} , d_{50} and d_{90} are the particle

122 diameters corresponding to, respectively, 10, 50 and 90 vol.% on a relative cumulative
123 particle size distribution curve (Vladisavljević and Schubert, 2003).

124 For the nanoparticle prodrug content determination, an aliquot of 4 ml of the nanoparticle
125 suspensions was collected and nanoparticles were washed twice with water through two
126 cycles of centrifugation at 14,610 *g* for 30 min (Eppendorf centrifuge 5804R). After the last
127 centrifugation, pellets were dissolved in 3 ml of EA and dried at 45°C under a nitrogen flow.
128 The dry residue was weighed and 3 ml EA was added. Then, 1.5 ml was collected and
129 centrifuged at 16,900 *g* for 30 min (Eppendorf centrifuge 5418R) and the supernatant was
130 collected for the prodrug spectrophotometric determinations as described in 2.2.4. For the
131 nanoparticle yield (weight%) determination, the weight of dry residue recovered from the 4
132 ml aliquot of nanoparticle suspension was used to calculate the total amount of nanoparticle
133 present in the initial 80 ml volume. The yield (weight%) was then calculated by dividing this
134 amount with the weight inputs of the prodrug or prodrug plus PLGA (*i.e.*, 200 mg in both
135 cases).

136

137 **2.2.2. Microparticle preparation**

138 The nanoparticle suspension was supplemented with L-leucine (2 mg/ml final concentration)
139 and centrifuged for 30 min at 14,610 *g* (Eppendorf centrifuge 5804R). The supernatant was
140 discarded and the pellet was re-dispersed in 20 ml of a solution of L-leucine (2 mg/ml) and
141 lactose (8 mg/ml), which corresponded to a nanoparticle-to-additive weight ratio ranging
142 from 0.60 to 0.85. Then the suspension was spray-dried using a Büchi® Mini Spray Dryer B-
143 290 (Switzerland) set up in blowing mode and equipped with a 0.7 mm nozzle. Settings were:
144 5% pump rate for the feed, air flow rate set at maximum level (13.65 l/min) and aspiration
145 rate of 100 %, with the pneumatic automatic nozzle cleaning operated 3 to 5 times per min.
146 The inlet and outlet temperatures were 81-83°C and 52-54°C, respectively. The obtained
147 powders were then characterized as described in 2.2.3.

148

149 **2.2.3. Microparticle characterization**

150 Scanning electron microscopy (SEM)

151 Microparticle powders were dispersed on double-sided adhesive carbon tapes that were
152 fixed on copper stubs and sputter coated with a platinum film. SEM images were taken using
153 a Teneo VolumeScope Electron microscope (FEI Thermo Scientific). The images were

154 obtained from the collection of secondary electrons under a voltage of 20 kV and a working
155 distance of 11 mm.

156

157 Aerodynamic diameter determination

158 The aerodynamic diameter was determined using a Next Generation Impactor (NGI, Copley
159 Ltd., Nottingham, UK), equipped with a TPK 2000 critical flow controller and a HCP5 vacuum
160 pump (Copley HCP5, Nottingham, UK) according to the European Pharmacopeia test
161 procedure 2.9.18. "Preparations for inhalation: aerodynamic assessment of fine particles" in
162 the conditions specified in the monograph "Preparations for inhalation (Inhalation
163 powders)", as previously described (Gaspar et al., 2015). For each measurement, a size-three
164 hard gelatin capsule was filled with 25 ± 1 mg of powder, inserted in a dry-powder inhaler
165 (DPI) Handihaler® (Boehringer-Ingelheim, Germany) and pierced according to the DPI user's
166 manual. The DPI was tightly connected to the NGI induction port via a silicone adapter. The
167 airflow rate was set at $41 \pm 5\%$ l/min in order to produce a pressure drop of 4 kPa through
168 the inhaler. The test duration time was set in order to draw 4 l of air through the inhaler. The
169 powder discharged from the capsule and deposited on the induction port, the stages and the
170 MOC filter was dissolved with EA for the prodrug spectrophotometric assay. Powder
171 deposited on the DPI and on the adapter was collected with ethanol, evaporated off at 45°C
172 under a nitrogen flow and the dry residue was dissolved in EA.

173 The emitted dose (ED), *i.e.* the mass of prodrug deposited in the induction port, the stages
174 and the MOC, was expressed as the percentage of the prodrug mass contained in the three
175 hard gelatin capsules. The percent cumulative mass fractions of prodrug deposited in MOC
176 and stages 1 to 7 were plotted versus the log aerodynamic diameters. The mass median
177 aerodynamic diameter (MMAD) was calculated by linear interpolation using the equation of
178 the linear interpolant that links the curve points immediately below and above 50%
179 deposition. The fine particle fraction (FPF) (*i.e.* the mass fraction of the prodrug within the
180 particles of 1-to-5 μm aerodynamic diameter) was expressed as the percentage of the ED.

181

182 Differential Thermal Analysis (DTA) and Thermal Gravimetric Analysis (TGA)

183 DTA and TGA were carried out on a SDT Q600 Instrument (TA Instruments, USA). Samples
184 placed on platinum pans were heated from 30°C to 350°C at a heating rate of 10°C/min
185 under a 100 ml/min air flow rate.

186

187 Prodrug content determination

188 For the prodrug extraction and quantification, 10 mg of microsphere powder (accurately
189 weighed) was dispersed in 1 mL EA. After dissolution of the prodrug, the mixture was
190 centrifuged at 14,610 g for 1 min (Eppendorf centrifuge 5804R). The supernatant was
191 collected for the prodrug spectrophotometric determinations as described in 2.2.4. The
192 prodrug content (%) was expressed as the amount of prodrug (mg) per 100 mg of
193 microsphere power.

194

195 In vitro release studies

196 For in vitro release studies under sink conditions, the microparticle powders (50 mg) were
197 dispersed in 10 ml of HBSS, pH 7.4, supplemented with 400 µl of a 1 mg/ml porcine lipase
198 solution in HBSS, and incubated at 37 °C under magnetic stirring (300 rpm) (Gaspar et al.,
199 2016). The lipase enzyme converted the released poorly water-soluble prodrugs into the
200 soluble parent drugs, which permitted to maintain sink conditions. At pre-determined time
201 points, aliquots were collected over 2 weeks and centrifuged at 16,900 g for 10 min
202 (Eppendorf centrifuge 5418R). Then, supernatants were collected and CHL and THA were
203 assayed by HPLC. In order to compensate for the loss of enzyme activity over time, the
204 porcine lipase solution (400µl) was added every day to the release medium.

205

206 **2.2.4. Prodrug spectrophotometric assay**

207 The nanoparticle or spray-dried powder prodrug contents (weight%), *i.e.* the amount of
208 prodrug (mg) per 100 mg of dry mass (including entrapped prodrug), were determined by
209 spectrophotometry at 273 nm using a Varian Cary 50 UV-Visible spectrophotometer after
210 dissolution in EA. The prodrug calibration curves in EA ranged from 3 to 60 µg/ml
211 concentration for CHLP and from 100 to 1000 µg/ml for THAP.

212

213 **2.2.5. Chloramphenicol and thiamphenicol HPLC assay**

214 The chromatographic system consisted of Waters 717 plus autosampler, a Hitachi L-7110
215 pump and a Eurosep 785 A spectrophotometric detector (Applied Biosystem). For CHL assay,
216 a C18 X Terra HPLC column (5 µm, 2.1x150 mm) with a Gemini C18 (4x2 mm) Phenomenex
217 precolumn was used. The mobile phase was composed of a 75:25 (v/v) acetonitrile: water

218 mixture supplemented with 0.1% (v/v) formic acid and 0.2% (v/v) PIC B7 and was run at a 0.2
219 ml/min flow rate. The injection volume, the run time and the detection wavelength were 50
220 μ l, 9 min and 275 nm, respectively. The calibration curve was constructed by linear
221 regression of the peak areas versus concentrations (0.125 - 10 μ g/ml in HBSS (pH 7.4)) with a
222 weighting factor of $1/x^2$ ($R^2 = 0.999$).

223 For THA determination, a C18 X Terra HPLC column (5 μ m, 3.9x150 mm) with a Gemini C18
224 (4x2 mm) Phenomenex precolumn was used. The mobile phase was composed of an 85:15
225 (v/v) acetonitrile: water mixture supplemented with 0.1% (v/v) formic acid and 0.2% (v/v)
226 PIC B7 and was run at a 0.4 ml/min flow rate. The injection volume, the run time and the
227 detection wavelength were 50 μ l, 18 min and 225 nm, respectively. The calibration curve
228 was constructed by linear regression of the peak areas versus concentrations (0.5 - 40 μ g/ml
229 in HBSS (pH 7.4)) with a weighting factor of $1/x^2$ ($R^2 = 0.999$).

230

231 **3. Results and discussion**

232 **3.1. Nanoparticle preparation**

233 A low molecular weight PLGA polymer with a rapid degradation rate (Diez and Tros de
234 Ilarduya, 2006; Gaspar et al., 2016) was used for the preparation of PLGA nanoparticles in
235 order to minimize the risk of polymer accumulation within the lung upon repeated dosing.
236 The prodrug content of the PLGA nanoparticles ranged from 50 to 60% (m/m), with a loading
237 efficiency of 100%, which indicated that the palmitate ester prodrugs had a high affinity for
238 the polymer (Table 1). This high entrapment efficiency is in agreement with previous works
239 where palmitate ester prodrugs were formulated within PLGA nanoparticles (Debotton et al.,
240 2008; Tangsumranjit et al., 2006). The entrapment efficiency within PLGA nanoparticles was
241 found to be dependent of the chain length of the carboxylic acid. Studying the effect of the
242 chain length of the carboxylate ligands (acetate to decanoate) of a platinum derivative,
243 Johnstone and Lippard showed a good correlation between the lipophilicity and the
244 entrapment efficiency within PLGA nanoparticles, with the highest efficiency for the
245 decanoate derivative (Johnstone and Lippard, 2013). In the case of dexamethasone acetate
246 (ester) prodrug, Gómez-Gaete et al observed that the prodrug was partially incorporated
247 within PLGA nanoparticles (Gomez-Gaete et al., 2008). It is interesting to note that using the
248 same procedure as for preparing prodrug-loaded PLGA nanoparticles, nanoparticles were
249 successfully prepared from pure CHLP or THAP prodrugs. Prodrug-loaded PLGA nanoparticles

250 and pure prodrug nanoparticles had virtually similar size, with a narrow size distribution
251 (span value below 1) and the mean yield ranged from 63 to 86 wt.%, which was considered
252 as satisfactory (Table 1). THAP-based nanoparticles were slightly larger than CHLP-based
253 ones.

254

255 **3.2. Dry microparticle powders**

256 Dry microparticle powders were obtained by spray-drying the nanoparticle aqueous
257 suspensions supplemented with lactose and L-leucine. The spray-drying production process
258 was reported to produce monodisperse microparticles with high encapsulation efficiency
259 and drug loading (Gomez-Gaete et al., 2008). Lactose was used as a bulking agent and L-
260 leucine as a dispersibility enhancer in order to obtain powders with appropriate
261 aerosolisation properties for inhaled delivery (Seville et al., 2007). Under 2,500x
262 magnification the dry powders appeared to be made of microparticles with diameter below
263 5 μm and were similar whatever the nanoparticles used (Fig. 2 and 3). In agreement with
264 reports showing that spray-dried powders are amorphous (Corrigan, 1995), no crystalline
265 structures like the CHLP or THAP crystals of the commercial prodrug powder (Fig. 1) were
266 observed on micrographs. Different from previous reported works (Gomez-Gaete et al.,
267 2008; Ruge et al., 2016; Torge et al., 2017), it was not possible to distinguish nanoparticles
268 even under the higher 10,000x and 40,000x magnifications. In these previous works the use
269 of a different bulking agent and of polymers with higher glass transition temperatures may
270 explain that the nanoparticle structures were preserved during the spray-drying process. The
271 microparticles appeared to be shriveled like raisin (Fig. 2 and 3). This typical shape was
272 attributed to the collapse of the microparticle structure during the spray-drying process and
273 was reported to be promoted by L-leucine (Seville et al., 2007; Yang et al., 2015). This is an
274 advantage for lung delivery, since particles with a high degree of surface corrugation were
275 shown to possess better aerosolisation properties due to reduced contact area (Adi et al.,
276 2008; Chew et al., 2005). Prodrug contents are presented in Table 2. As expected, the
277 prodrug content was higher when the spray-dried powders were obtained from
278 nanoparticles made of pure prodrugs, than with the prodrug-loaded PLGA nanoparticles.

279

280 **3.3. DTA-TGA analysis**

281 DTA-TGA analysis was conducted to analyze the interaction between CHLP and THAP with
282 PLGA, L-leucine and lactose. Thermograms of CHL and THA (Fig. 4A and 4B) showed
283 endothermic peaks at 153.6°C and 167.1°C corresponding to their respective melting points
284 (Aiassa et al., 2015). Thermal degradation occurred at an onset temperature of around 200°C
285 for CHL and THA as shown by the exothermic peaks (Fig. 4A and 4B) and the gradual weight
286 loss (Fig. 4C and 4D). The prodrug CHLP exists as three described polymorphs: the stable
287 form A and two metastable forms B and C (Kaneniwa and Otsuka, 1985), with different
288 solubility values and oral bioavailability. Forms B and C are suitable for therapeutic use, but
289 form A is considered as biologically inactive, which was attributed to a different
290 susceptibility to pancreatic lipase in the upper intestinal tract. Forms A and B have respective
291 melting points at 90.3 or 92°C and 86.7 °C respectively (Gamberini et al., 2006; Kaneniwa
292 and Otsuka, 1985). The endothermic peak at 88.3°C on the CHLP thermogram (Fig. 4A) may
293 correspond to form B or a mix of forms A and B, since the metastable form B tends to
294 transform into the stable form A (Gamberini et al., 2006). The thermogram of THAP (Fig. 4B)
295 showed an endothermic peak at 111.3°C which was attributed to its melting point. For both
296 prodrugs, degradation occurred with an onset at around 230°C (Fig. 4A and 4B), as deduced
297 from the exothermic peaks and from the weight loss (Fig. 4C and 4D).

298 For the four microparticle powders, the weight loss of 2 to 5 % observed over 40 to 70°C
299 (Fig. 4C and 4D) was due to the evaporation of residual water (Raula et al., 2012). A further
300 weight loss with an onset at around 140°C was simultaneous with an endothermic event
301 (over 145 to 190°C) and was attributed to the sublimation of the L-leucine (Lähde et al.,
302 2009). The exothermic event with an onset at 190-200°C (Fig. 4A and 4B) which is
303 simultaneous with an important weight loss (Fig. 4C and 4D) was attributed to the thermal
304 degradation of the microparticle components. The thermograms of microparticle powders
305 made with CHLP nanoparticles or with CHLP-loaded PLGA nanoparticles were roughly similar
306 (Fig. 4A) with a small endothermic peak at 85.8°C attributed to the melting of the CHLP
307 crystal form B. The small size of this endothermic peak suggests that CHLP is mainly in an
308 amorphous or solubilized form. Microparticle powders made with THAP nanoparticles or
309 THAP-loaded PLGA nanoparticles showed also similar thermograms (Fig. 4 C&D). The small
310 endothermic peak at 108-109°C was attributed to the melting of THAP (see the pure THAP
311 thermogram as a reference) and, taking into account the microsphere THAP content, its size
312 indicates that THAP is mainly in an amorphous or solubilized form.

313

314 **3.4. Aerodynamic properties**

315 For all the formulations, the high ED% values (above 70%) indicated that the microparticle
316 powders were efficiently emitted from the DPI (Table 2). MMAD values were around 3 μm ,
317 suggesting that the microparticles powders successfully de-aggregated during the
318 aerosolisation process within the DPI. FPF (%) were very satisfactory in the range of values
319 reported for marketed formulations (15-30%) for pulmonary administration (Smith and
320 Parry-Billings, 2003), indicating that the powders should be efficient to deliver CHLP and
321 THAP to the lungs through inhalation. With MMAD around 3 μm microparticles mainly
322 deposit in the central airway, where bacteria are difficult to eradicate using systemic
323 administration of antibiotics due to a low vascularization, thicker epithelium, mucus and
324 biofilm formation, compared to alveoli (Bjarnsholt et al., 2009).

325

326 **3.5. Prodrug release studies**

327 Prodrug release studies were carried out at 37°C in HBSS buffer, pH 7.4. In order to maintain
328 sink conditions, porcine lipase was added to the release medium, which converted the
329 poorly soluble prodrugs released in HBSS buffer into the more soluble parent drugs, which
330 were eventually determined by HPLC. In the case of the microparticle powder formulations
331 prepared with CHLP- nanoparticles (with or without PLGA), the release profiles were rather
332 linear and showed a sustained release of the prodrugs (Fig 5) with 70 (without PLGA) or 90%
333 (with PLGA) release at 14 days.

334 With the THAP powders, the profiles were characterized with a two-rate release. A higher
335 rate over 3 or 4 days with 60% or 50% cumulated release without or with PLGA respectively,
336 followed by lower rate resulting in 80% cumulated release at 14 days. This was attributed to
337 the higher water solubility of the THA moiety than the solubility of the CHL moiety, leading
338 to a higher dissolution rate in the release medium. Release rates were also higher with the
339 microparticle powders made with prodrug-loaded PLGA nanoparticles than with those made
340 with pure prodrug nanoparticles. In the case of prodrug-loaded PLGA nanoparticles,
341 prodrugs are dispersed within the PLGA matrix that gradually degrades. Such degradation is
342 likely to produce pores within the nanoparticles that permit the entry of water and increase
343 the exchange surface area with the release medium.

344 For both prodrugs, whatever the formulation, the releases were much slower than in
345 previously reported results obtained with dexamethasone acetate-loaded PLGA
346 nanoparticles (Gomez-Gaete et al., 2008). This can be explained by a higher affinity of the
347 CHLP or THAP prodrugs towards the PLGA polymer, resulting in a slower drug release.
348 It is difficult to anticipate whether such relatively slow sustained release profiles of the
349 prodrugs and their hydrolysis rate into the active drugs within the lungs will be appropriate
350 to reach efficient CHL or THA concentrations in the lung areas. Previous PK studies with
351 sustained release rifampicin or levofloxacin-loaded PLGA microparticles showed that such
352 delivery systems permitted to reach high epithelial lining fluid (ELF) to blood plasma drug
353 concentration ratios due to the local release in the small ELF volume. In addition, little is
354 known about the esterase activity within the lungs (Camps et al., 1991). Therefore, PK
355 studies will be necessary to further investigate the therapeutic potential of the present
356 formulations.

357

358 **4. Conclusion**

359 Dry powder formulations of CHLP or THAP with sustained release profiles and appropriate
360 aerodynamic properties for lung delivery as aerosols were successfully prepared with the
361 nanoparticle-within- microparticle spray-drying production technology. Further PK
362 investigations are needed to evaluate the potential efficiency of such innovative CHLP or
363 THAP drug delivery systems.

364

365 **Acknowledgements**

366 The authors thank the Directorate General of Higher Education (DGHE) of Indonesia for the
367 financial support of Nurbaeti S.N. (the funders had no role in study design, data collection
368 and interpretation, or the decision to submit the work for publication). DTA/TGA analyses
369 were performed at the University of Poitiers Pôle Commun de Mesures Physico-chimiques
370 platform. SEM imaging was performed at the University of Poitiers imaging platform
371 ImageUP. Spray-drying experiments were carried out in Biocydex, Poitiers. The authors
372 thank Ms. Agnès Audurier, INSERM U 1070 and Faculty of Medicine and Pharmacy, for her
373 technical assistance, and Mr. Patrice Godin and Mr. Christophe Adier, INSERM U 1070 and
374 CHU de Poitiers, for their technical assistance in the spectrophotometric and HPLC
375 determinations and the Quality Management of the analytical process.

376

377 **Conflict of interest**

378 The authors report no conflicts of interest.

379

380

381 **References**

382

383 Adi, S., Adi, H., Tang, P., Traini, D., Chan, H.K., Young, P.M., 2008. Micro-particle corrugation,
384 adhesion and inhalation aerosol efficiency. *European journal of pharmaceutical sciences : official*
385 *journal of the European Federation for Pharmaceutical Sciences* 35, 12-18.

386 Aiassa, V., Zoppi, A., Albesa, I., Longhi, M.R., 2015. Inclusion complexes of chloramphenicol with
387 beta-cyclodextrin and aminoacids as a way to increase drug solubility and modulate ROS production.
388 *Carbohydrate polymers* 121, 320-327.

389 Ambrose, P.J., 1984. Clinical pharmacokinetics of chloramphenicol and chloramphenicol succinate.
390 *Clinical pharmacokinetics* 9, 222-238.

391 Bjarnsholt, T., Jensen, P.Ø., Fiandaca, M.J., Pedersen, J., Hansen, C.R., Andersen, C.B., Pressler, T.,
392 Givskov, M., Høiby, N., 2009. *Pseudomonas aeruginosa* biofilms in the respiratory tract of cystic
393 fibrosis patients. *Pediatric pulmonology* 44, 547-558.

394 Camps, L., Reina, M., Llobera, M., Bengtsson-Olivecrona, G., Olivecrona, T., Vilaro, S., 1991.
395 Lipoprotein lipase in lungs, spleen, and liver: synthesis and distribution. *Journal of lipid research* 32,
396 1877-1888.

397 Chew, N.Y., Tang, P., Chan, H.K., Raper, J.A., 2005. How much particle surface corrugation is sufficient
398 to improve aerosol performance of powders? *Pharmaceutical research* 22, 148-152.

399 Corrigan, O.I., 1995. Thermal analysis of spray dried products. *Thermochimica Acta* 248, 245-258.

400 Debotton, N., Parnes, M., Kadouche, J., Benita, S., 2008. Overcoming the formulation obstacles
401 towards targeted chemotherapy: in vitro and in vivo evaluation of cytotoxic drug loaded
402 immunonanoparticles. *Journal of controlled release : official journal of the Controlled Release Society*
403 127, 219-230.

404 Diez, S., Tros de Ilarduya, C., 2006. Versatility of biodegradable poly(D,L-lactic-co-glycolic acid)
405 microspheres for plasmid DNA delivery. *European journal of pharmaceuticals and biopharmaceutics :*
406 *official journal of Arbeitsgemeinschaft fur Pharmazeutische Verfahrenstechnik e.V* 63, 188-197.

407 Dinos, G.P., Athanassopoulos, C.M., Missiri, D.A., Giannopoulou, P.C., Vlachogiannis, I.A.,
408 Papadopoulos, G.E., Papaioannou, D., Kalpaxis, D.L., 2016. Chloramphenicol Derivatives as
409 Antibacterial and Anticancer Agents: Historic Problems and Current Solutions. *Antibiotics (Basel,*
410 *Switzerland)* 5.

411 Doan, T.V., Gregoire, N., Lamarche, I., Gobin, P., Marchand, S., Couet, W., Olivier, J.C., 2013. A
412 preclinical pharmacokinetic modeling approach to the biopharmaceutical characterization of
413 immediate and microsphere-based sustained release pulmonary formulations of rifampicin.
414 *European journal of pharmaceutical sciences : official journal of the European Federation for*
415 *Pharmaceutical Sciences* 48, 223-230.

416 Eliakim-Raz, N., Lador, A., Leibovici-Weissman, Y., Elbaz, M., Paul, M., Leibovici, L., 2015. Efficacy and
417 safety of chloramphenicol: joining the revival of old antibiotics? *Systematic review and meta-analysis*
418 *of randomized controlled trials. The Journal of antimicrobial chemotherapy* 70, 979-996.

419 Ferrari, V., 1984. Salient features of thiamphenicol: review of clinical pharmacokinetics and toxicity.
420 *Sexually transmitted diseases* 11, 336-339.

421 Gamberini, M.C., Baraldi, C., Tinti, A., Rustichelli, C., Ferioli, V., Gamberini, G., 2006. Solid state
422 characterization of chloramphenicol palmitate. Raman spectroscopy applied to pharmaceutical
423 polymorphs. *Journal of Molecular Structure* 785, 216-224.

424 Gaspar, M.C., Gregoire, N., Sousa, J.J., Pais, A.A., Lamarche, I., Gobin, P., Olivier, J.C., Marchand, S.,
425 Couet, W., 2016. Pulmonary pharmacokinetics of levofloxacin in rats after aerosolization of
426 immediate-release chitosan or sustained-release PLGA microspheres. *European journal of*
427 *pharmaceutical sciences : official journal of the European Federation for Pharmaceutical Sciences* 93,
428 184-191.

429 Gaspar, M.C., Sousa, J.J., Pais, A.A., Cardoso, O., Murtinho, D., Serra, M.E., Tewes, F., Olivier, J.C.,
430 2015. Optimization of levofloxacin-loaded crosslinked chitosan microspheres for inhaled aerosol

431 therapy. *European journal of pharmaceutics and biopharmaceutics : official journal of*
432 *Arbeitsgemeinschaft fur Pharmazeutische Verfahrenstechnik e.V* 96, 65-75.

433 Gomez-Gaete, C., Fattal, E., Silva, L., Besnard, M., Tsapis, N., 2008. Dexamethasone acetate
434 encapsulation into Trojan particles. *Journal of controlled release : official journal of the Controlled*
435 *Release Society* 128, 41-49.

436 Han, J., Michel, A.R., Lee, H.S., Kalscheuer, S., Wohl, A., Hoyer, T.R., McCormick, A.V., Panyam, J.,
437 Macosko, C.W., 2015. Nanoparticles Containing High Loads of Paclitaxel-Silicate Prodrugs:
438 Formulation, Drug Release, and Anticancer Efficacy. *Molecular pharmaceutics* 12, 4329-4335.

439 Johnstone, T.C., Lippard, S.J., 2013. The effect of ligand lipophilicity on the nanoparticle
440 encapsulation of Pt(IV) prodrugs. *Inorganic chemistry* 52, 9915-9920.

441 Kaneniwa, N., Otsuka, M., 1985. Effect of grinding on the transformations of polymorphs of
442 chloramphenicol palmitate. *Chemical and pharmaceutical bulletin* 33, 1660-1668.

443 Lähde, A., Raula, J., Malm, J., Kauppinen, E.I., Karppinen, M., 2009. Sublimation and vapour pressure
444 estimation of l-leucine using thermogravimetric analysis. *Thermochimica Acta* 482, 17-20.

445 Lam, R., Lai, J., Ng, J., Rao, S., Law, R., Lam, D., 2002. Topical chloramphenicol for eye infections. *Hong*
446 *Kong medical journal= Xianggang yi xue za zhi* 8, 44-47.

447 Macchi, A., Terranova, P., Macchi, S., Roselli, R., Castelnovo, P., 2011. Aerosol therapy with
448 thiamphenicol glycinate: a retrospective study on efficacy and safety in a group of sixty-six
449 oncological patients. *International journal of immunopathology and pharmacology* 24, 189-193.

450 Nurbaeti, S.N., Olivier, J.-C., Adier, C., Marchand, S., Couet, W., Brillault, J., 2018. Active Mediated
451 Transport of Chloramphenicol and Thiamphenicol in a Calu-3 Lung Epithelial Cell Model. *Journal of*
452 *pharmaceutical sciences* 107, 1178-1184.

453 Pulcini, C., Mohrs, S., Beovic, B., Gyssens, I., Theuretzbacher, U., Cars, O., Bosevska, G., Bruch, M.,
454 Bush, K., Cizmovic, L., 2017. Forgotten antibiotics: a follow-up inventory study in Europe, the USA,
455 Canada and Australia. *International journal of antimicrobial agents* 49, 98-101.

456 Raula, J., Seppälä, J., Malm, J., Karppinen, M., Kauppinen, E.I., 2012. Structure and dissolution of l-
457 leucine-coated salbutamol sulphate aerosol particles. *AAPS PharmSciTech* 13, 707-712.

458 Ruge, C.A., Bohr, A., Beck-Broichsitter, M., Nicolas, V., Tsapis, N., Fattal, E., 2016. Disintegration of
459 nano-embedded microparticles after deposition on mucus: A mechanistic study. *Colloids and*
460 *Surfaces B: Biointerfaces* 139, 219-227.

461 Serra, A., Schito, G., Nicoletti, G., Fadda, G., 2007. A therapeutic approach in the treatment of
462 infections of the upper airways: thiamphenicol glycinate acetylcysteinate in sequential treatment
463 (systemic-inhalatory route). *International journal of immunopathology and pharmacology* 20, 607-
464 617.

465 Seville, P., Learoyd, T., Li, H.-Y., Williamson, I., Birchall, J., 2007. Amino acid-modified spray-dried
466 powders with enhanced aerosolisation properties for pulmonary drug delivery. *Powder technology*
467 178, 40-50.

468 Smith, I.J., Parry-Billings, M., 2003. The inhalers of the future? A review of dry powder devices on the
469 market today. *Pulmonary pharmacology & therapeutics* 16, 79-95.

470 Tangsumranjit, A., Pellequer, Y., Lboutounne, H., Guillaume, Y., Lamprecht, A., Millet, J., 2006.
471 Enhanced ascorbyl palmitate stability by polymeric nanoparticles. *Journal of drug delivery science*
472 *and technology* 16, 161-163.

473 Tetko, I.V., Gasteiger, J., Todeschini, R., Mauri, A., Livingstone, D., Ertl, P., Palyulin, V.A., Radchenko,
474 E.V., Zefirov, N.S., Makarenko, A.S., Tanchuk, V.Y., Prokopenko, V.V., 2005. Virtual computational
475 chemistry laboratory--design and description. *Journal of computer-aided molecular design* 19, 453-
476 463.

477 Torge, A., Grützmacher, P., Mücklich, F., Schneider, M., 2017. The influence of mannitol on
478 morphology and disintegration of spray-dried nano-embedded microparticles. *European Journal of*
479 *Pharmaceutical Sciences* 104, 171-179.

480 Vladislavljević, G.T., Schubert, H., 2003. Influence of process parameters on droplet size distribution in
481 SPG membrane emulsification and stability of prepared emulsion droplets. *Journal of Membrane*
482 *Science* 225, 15-23.

483 Yang, F., Liu, X., Wang, W., Liu, C., Quan, L., Liao, Y., 2015. The effects of surface morphology on the
 484 aerosol performance of spray-dried particles within HFA 134a based metered dose formulations.
 485 asian journal of pharmaceutical sciences 10, 513-519.
 486 Yunis, A.A., 1984. Differential in-vitro toxicity of chloramphenicol, nitroso-chloramphenicol, and
 487 thiamphenicol. Sexually transmitted diseases 11, 340-342.

488

489 **Table 1:** Characterization of nanoparticles (mean±SD, n = 8-9)

Nanoparticle type	Dv (nm) of the PSD	Span of the PSD ¹	Prodrug content (% m/m) ²	Yield (%)	490	491	492	493	494	495	496	497	498	¹ PS	D: particle size distribution
CHLP nanoparticles	159±6	0.54±0.07	82±11	86±5											
CHLP-loaded PLGA nanoparticles	160±4	0.64±0.09	50±13	63±18											
THAP nanoparticles	177±6	0.79±0.07	91±22	84±9											
THAP-loaded PLGA nanoparticles	178±12	0.77±0.04	60±14	70±7											

499 prodrug per 100 mg nanoparticle

500

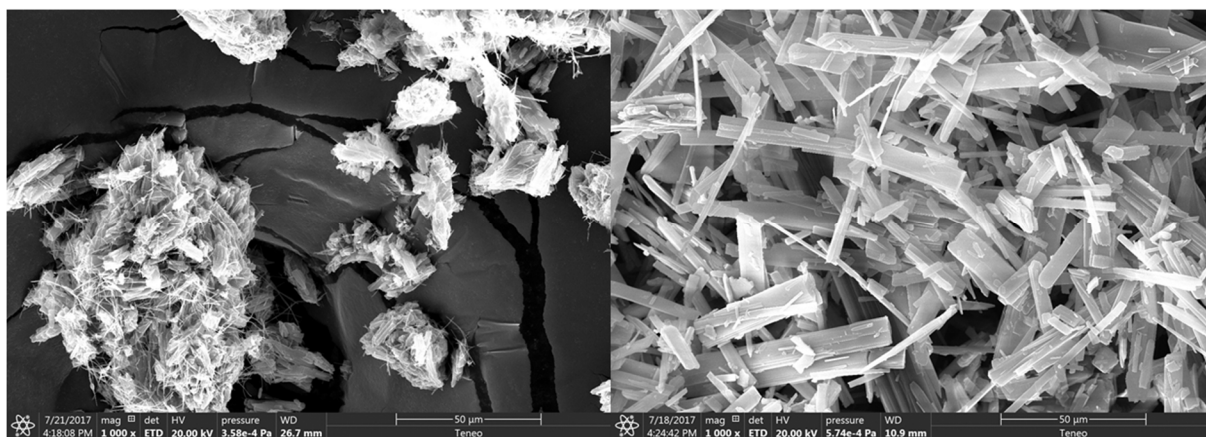
501

502 **Table 2:** Prodrug contents and aerodynamic characterization of the dry microparticle
 503 powders (mean±SD, n = 3-4)

Dry microparticle powder made with :	Prodrug content (% m/m) ¹	ED (%)	FPF (%) (1-5µm)	MMAD (µm)
CHLP nanoparticles	30.2±1.0	75±9	33±10	3.1±0.2
CHLP-loaded PLGA nanoparticles	13.9±3.0	79±8	27±13	3.3±0.5
THAP nanoparticles	34.5±4.8	91±8	47±9	2.9±0.2
THAP-loaded PLGA nanoparticles	21.0±0.7	82±19	36±10	2.8±0.3

504 ¹mg prodrug per 100 mg dry microparticle powder

505

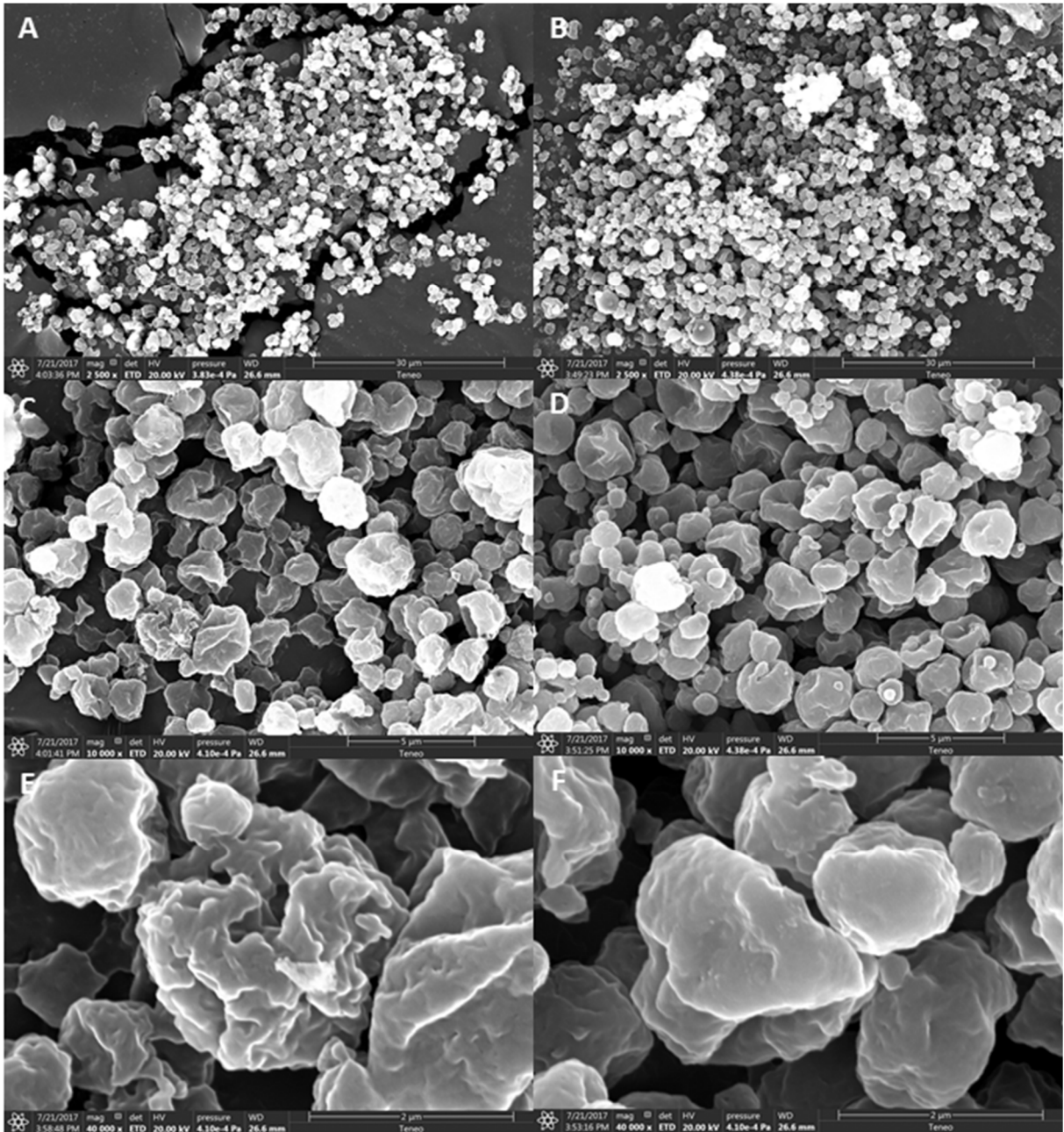


506

507 **Figure 1:** SEM of the commercial CHLP (left) and THAP (right) powders

508

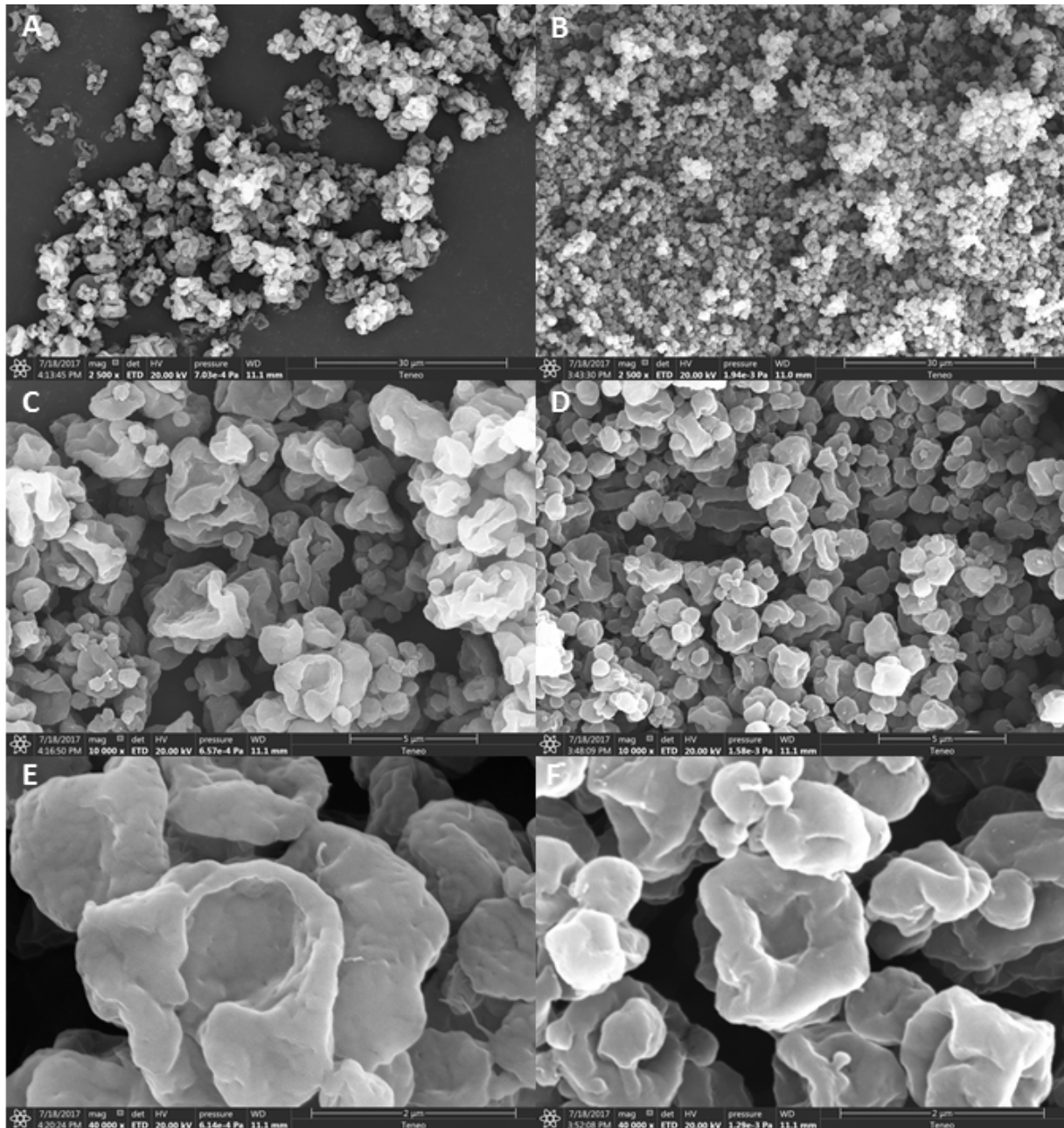
509



510

511 **Figure 2:** SEM of microparticle powders prepared with CHLP nanoparticles (A, C and E) or
512 CHLP-loaded PLGA nanoparticles (B, D and E) with magnifications of 2,500x for A and B,
513 10,000x for C and D and 40,000x for E and F.

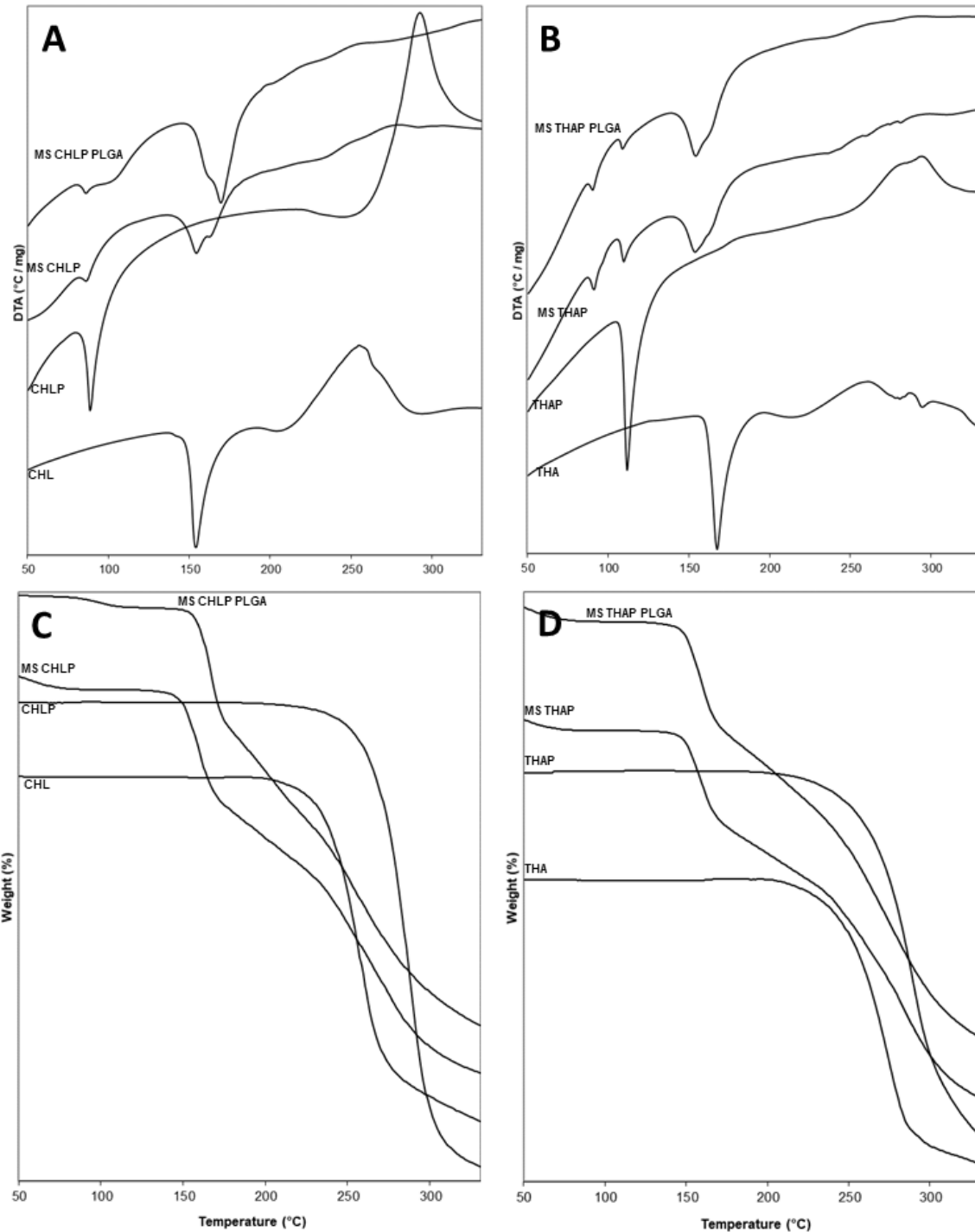
514



515

516 **Figure 3:** SEM of microparticle powders prepared with THAP nanoparticles (A, C and E) or
 517 THAP-loaded PLGA nanoparticles (B, D and F) with magnifications of 2,500x for A and B,
 518 10,000x for C and D and 40,000x for E and F.

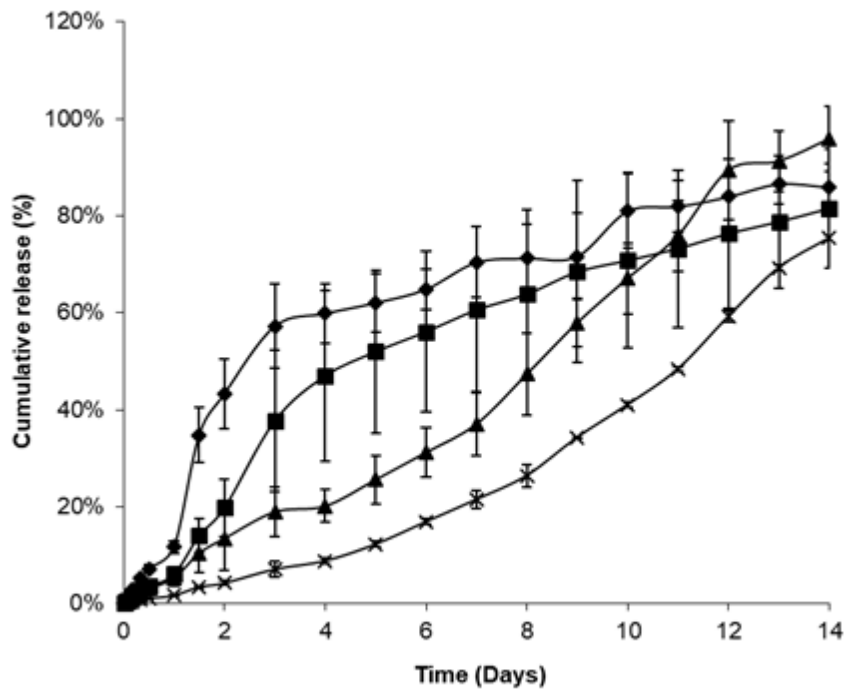
519



520

521 **Figure 4:** DTA (A & B) and TGA (C & D) thermograms of raw materials (CHL, CHLP, THA and
 522 THAP) and of dry microparticle powders made with CHLP or THAP nanoparticles (MS CHLP or
 523 MS THAP) or with CHLP- or THAP-loaded PLGA nanoparticles (MS PLGA CHLP or MS PLGA
 524 THAP). Total weight loss (%) is indicated on TGA curves.

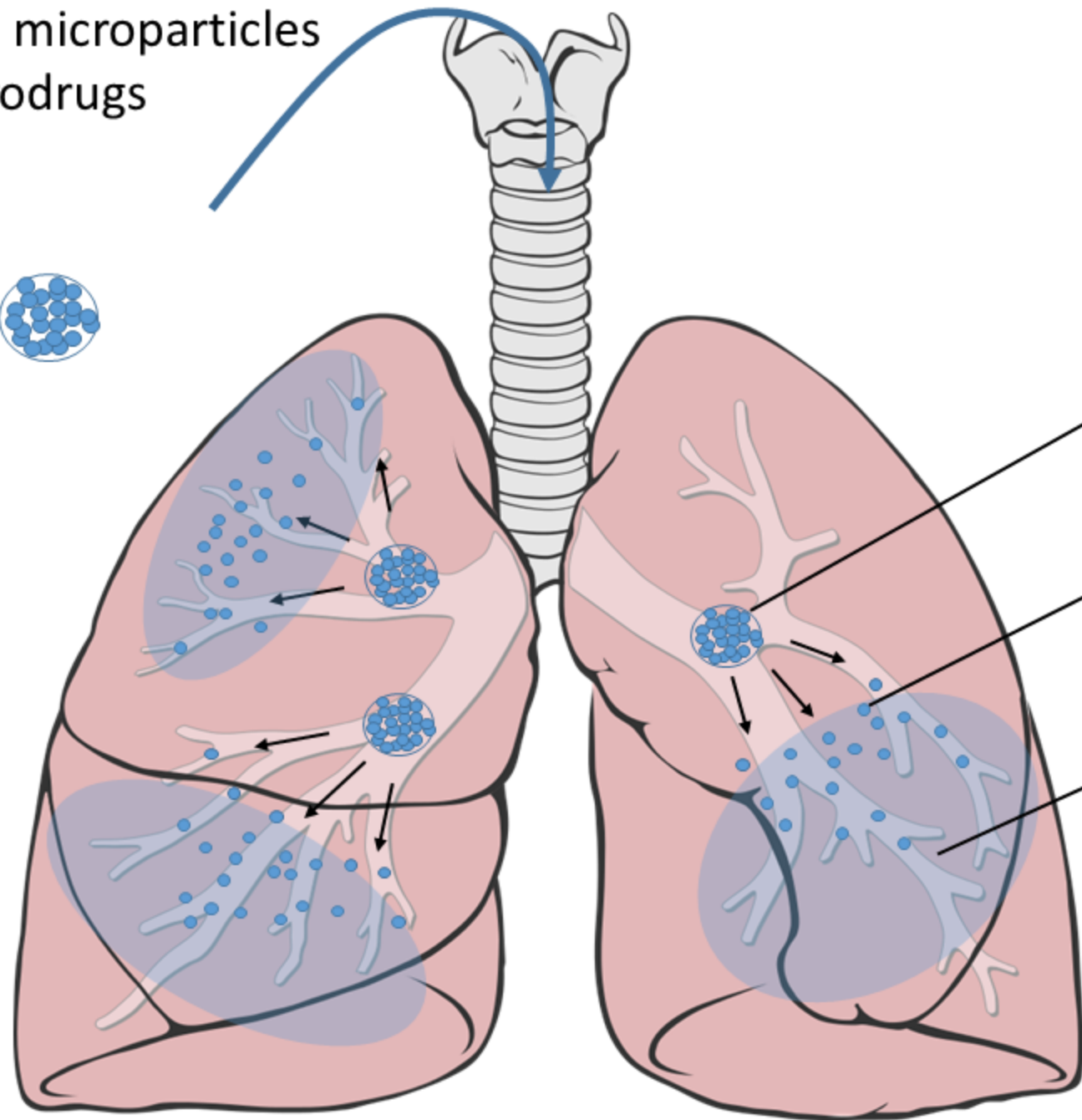
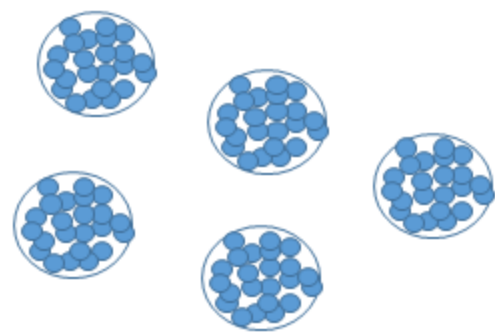
525



526

527 **Figure 5:** In vitro prodrug release profiles in HBSS medium, 37°C, for dry microparticle
 528 powders made with CHLP nanoparticles (x), with THAP nanoparticles (■), with CHLP-loaded
 529 PLGA nanoparticles (▲) or with THAP-loaded PLGA nanoparticles (◆).

Inhalable nano-embedded microparticles of amphenicol prodrugs



3 μm diameter microparticles

160 nm diameter nanoparticles

controlled release of amphenicol prodrugs